

An effective magnetic field from optically driven phonons

T. F. Nova¹, A. Cartella¹, A. Cantaluppi¹, M. Först¹, D. Bossini², R. V. Mikhaylovskiy², A.V.

Kimel², R. Merlin³ and A. Cavalleri^{1,4}

¹Max Planck Institute for the Structure and Dynamics of Matter, 22761 Hamburg, Germany

²Radboud University, Institute for Molecules and Materials, 6525 AJ Nijmegen, The Netherlands

³Department of Physics, University of Michigan, Ann Arbor, Michigan 48109-1040, USA

⁴University of Oxford, Clarendon Laboratory, Oxford OX1 3PU, UK

Circularly polarized optical pulses have been shown to induce a breaking of time reversal invariance in solids, allowing for the control of magnetism through electronic Raman scattering. Here, we combine this principle with elements of magnetoelastics, and show that optical excitation of pairs of infrared-active optical phonons can excite coherent spin waves in the rare-earth orthoferrite ErFeO₃. This phenomenon relies on the real-space rotations of the crystal-field atoms and on the resulting effective magnetic field onto the Fe³⁺ orbitals. Coherent control of lattice rotations could be used not only in magnetic solids, but more generally in materials with interesting topological properties.

Light fields at THz and mid-infrared frequencies allow for the direct excitation of collective modes of condensed matter, which can be driven to large amplitudes and into their nonlinear response regime. Amongst many examples of such mode-selective control, coherent *nonlinear phononics*ⁱ has emerged as a new means to manipulate the solid state. Coherent coupling between anharmonically coupled phonons has been used to deform the crystal structure along selected coordinates, and has been shown to stimulate insulator-metal transitions^{ii,iii}, to melt magnetic order^{iv,v} and to enhance superconductivity^{vi,vii,viii}.

Here, we generalize the idea of nonlinear phononics^{ix} and show that the excitation of pairs of non-degenerate vibrations can drive atomic rotations as well as displacements. This breaking of time reversal invariance through lattice rotations mimics the application of a magnetic field and is manifested here in the excitation of large amplitude spin precession in a rare-earth orthoferrite. This unusual breaking of time reversal invariance through the lattice can be achieved by virtue of the mutual coherence of these phonon modes, and is shown here to drive precession in different directions depending on the relative phase between the two excited phonons.

ErFeO₃ is an antiferromagnetic insulator that crystallizes in an orthorhombically distorted perovskite structure, as shown in Fig. 1a (space group: Pbnm). Because of the Dzyaloshinskii-Moryia^{x,xi} interaction, the spins are canted along the *c* direction and result in a small ferromagnetic moment along the *c* axis (Fig. 1b). In our experiments, femtosecond mid-IR pulses were tuned to drive the highest-frequency in-plane B_{ua} and B_{ub} phonons (Fig. 1c). The pump was linearly polarized and aligned at a variable angle with respect to the *a* and *b* crystallographic axes. Depending on this

alignment, only one or both phonon modes could be excited and their relative phase could be changed by aligning the pump pulse at +45 or -45 degrees.

Because of the orthorhombic distortion of ErFeO_3 , these two modes are singly degenerate and exhibit different eigenfrequencies (ν_a and ν_b). Hence, when the two lattice vibrations are excited simultaneously (e.g. with the light polarization at 45 degrees angle from either crystal axes), the relative phase between the two modes advances in time. This dephasing causes the ions to rotate about their equilibrium position, as shown in Fig. 1d. The lighter O^{2-} ions, which dominate the crystal field applied on the high-spin Fe^{3+} ions, trace elliptical orbits with eccentricity that increases in time. This eccentricity reverses after an interval $T = 1/[2(\nu_a - \nu_b)]$ (see Fig. 1e). However, because of damping, the amplitude of the two vibrational modes and the area of the orbit reduce in time. Hence, for certain combinations of phonon frequency differences and damping rates, the initial rotational direction dominates the coherent response resulting in a net breaking of time reversal invariance.

To find evidence for such an effect, we measured the Faraday rotation of a linearly polarized near infrared (800-nm wavelength) probe pulse after transmission through the sample as a function of time delay following lattice excitation (see S1). As shown in Figure 2a, the time dependent polarization rotation oscillated in time, revealing the coherent excitation of a number of Raman active modes (Fig. 2b). These included Raman $A_{1g} + B_{1g}$ and B_{1g} (3.36 THz and 4.86 THz) phonons and, most strikingly, a Raman-active quasi-antiferromagnetic magnon (q-AFM, 0.75 THz)^{xii}, associated with an oscillatory ferromagnetic moment along the c axis (Fig. 2c)^{xiii}.

Fig. 3a displays the pump wavelength dependence of the total magnetization change, extracted from the raw data by normalizing against the difference in

penetration depth between the pump and the probe pulses (see S5). The coherent magnon amplitude, small in the polariton regime at frequencies above the LO phonon resonances (i.e. above 20 THz), was strongly enhanced for wavelengths within the Reststrahlen band. Note that in this spectral region the real part of the dielectric permittivity of the material becomes negative, and light couples coherently to an evanescent mechanical wave. The ions oscillate to screen the incoming light, and to linear order no absorption or dissipation takes place.

The maximum lattice-induced precession amplitude for excitation within the Reststrahlen band corresponds here to a 1.5% change of the saturation magnetization, comparable to what was achieved by off-resonant excitation with circularly polarized light^{xiv}.

We also measured the pump-field dependence of the coherent magnetization dynamics (Fig. 3b). The magnon amplitude was found to scale quadratically with the electric field strength of the pump. Hence, the response is proportional to the product of two phonon coordinates.

Coherent magnon oscillations were only observed for pump pulses polarized at +45 or – 45 degrees, in between the crystallographic *a* and *b* axes (Fig. 4a, red and orange lines). When the pump electric field was directed along either of the crystallographic axes, only Raman phonons were detected (Fig. 4a, blue and grey lines). We thus conclude that the magnetic response is observed only when both phonon modes are excited. Furthermore, the phase of the magnon oscillations switches sign when the pump polarization is rotated from +45 degrees to – 45 degrees, revealing a dependence on the relative phase of the two driven phonons (Fig. 4a, red and orange lines).

Finally, the phase of the measured magnon oscillations did not change when the static magnetization was reversed (Fig. 4b), indicating that the direction of the magnetic oscillations was independent from the initial canting of the spins.

These observations indicate that the mixing of pairs of phonons results in an effective magnetic field. Let us consider the physical situation depicted in Figure 1d, where the oxygen ions perform rotational motions. Qualitatively, this dynamics is expected to modify the crystal field felt by the Fe^{3+} ion at the centre of the octahedron. This effect mixes the ground state $t_{2g}^3 e_g^2$ electronic wavefunction^{xv} at each Fe^{3+} ion, which has negligible spin orbit interaction, with excited states, for which spin-orbit coupling is enhanced. Thus, the electric field of the moving ions promptly perturbs the angular momentum of the $t_{2g}^3 e_g^2$, effectively activating spin-orbit interactions in the ground state and hence triggering a magnetic excitation.

In analogy with what has been discussed in the case of electronic Raman excitation of magnons^{xvi, xvii, xviii, xix}, our results can be described by considering an effective Hamiltonian of the form $H_{eff} = i\alpha_{abc} Q_{ua} Q_{ub}^* M_c$. In this expression, α_{abc} is the magneto-elastic susceptibility, antisymmetric over the first pair of indices $\alpha_{abc} = -\alpha_{bac}$, Q_{ua} and Q_{ub}^* are the phonon eigenvectors and M_c is the static magnetization.

Hence, the circularly polarized lattice motion behaves as an effective magnetic field

$$\left[-\frac{\partial H_{eff}}{\partial M_c} \right] = -i\alpha_{abc} Q_{ua} Q_{ub}^*$$

directed perpendicular to the rotation plane.

Furthermore, the sign of the field depends on the rotation direction of the ions. This explains why a 90 degrees change in the pump polarization, that is a sign change in the initial phase of one of the two IR-active phonons, results in a π phase shift in the

magnon (Fig. 4b). In fact, the initial phase of the phonons determines the initial helicity of the ionic loops (Fig. 1e) and therefore the sign of the effective field.

In general, the spin precession is expected to be impulsively excited in all cases in which the initial rate of change of the effective magnetic field is prompt compared to the period of the magnon.

However, note also that for specific wavelengths throughout the Reststrahlen band (e.g. near the TOs frequency), the two phonons can be excited with a frequency difference $\Delta\nu_{TO} = 17.03 \text{ THz} - 16.17 \text{ THz} = 0.86 \text{ THz}$ that matches that of the magnon $\nu_{magnon} = 0.75 \text{ THz}$ thus resulting in a resonant driving of the latter by the effective magnetic field. This suggests a scenario in which magnetism can be excited using pairs of continuous wave mid-infrared pumps, extending our results to quasi-static experimental conditions.

We also note that due to the nonlinear nature of the excitation mechanism, which depends on the product of the driven phonon coordinates, a moderate increase in the field strength may drive the magnetic amplitude beyond the few percent observed here, into the nonlinear response and possibly toward magnetic switching. Although the response is of similar magnitude as that observed when using near-infrared optical pulses, the current principle may allow for smaller dissipation. Optical experiments performed even in the transparency region and below gap, are prone to dissipation due to multi-photon absorption, whereas the mechanical coupling achieved here is expected to scale better with high fields. Importantly, the mechanism exploited here relies on the application of effective magnetic fields but does not require pre-existing multiferroicity^{xx,xxi,xxii}, and may even be used to control the properties of non-magnetic oxides. Finally, beyond the applications to

magnetism discussed here, we note that control of ionic loops can be viewed as a perturbation of the Berry connection^{xxiii,xxiv}, and in appropriate circumstances may be used to manipulate the topological properties of materials^{xxv}.

FIGURES

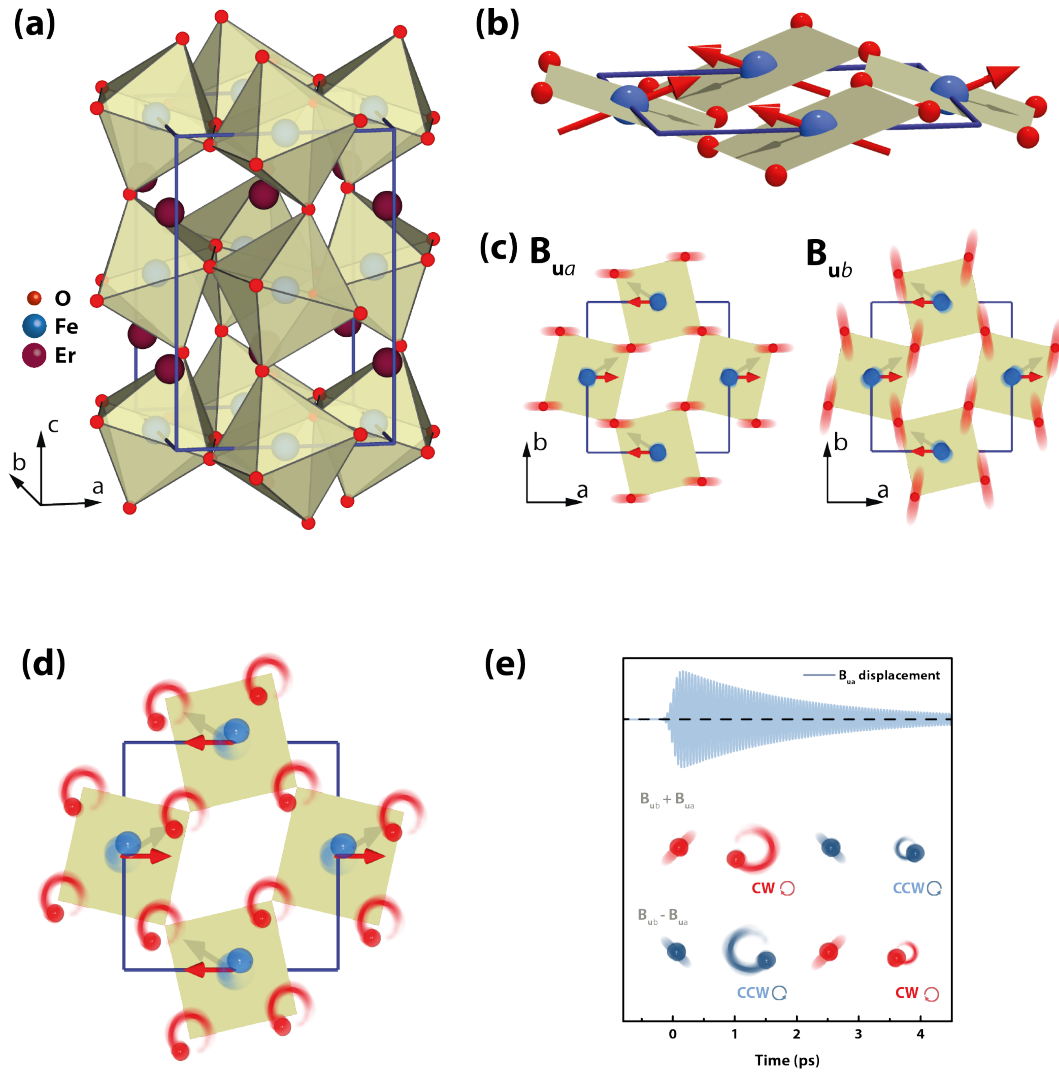


Figure 1 (a) Crystal structure of ErFeO_3 , an orthorhombically distorted perovskite (Pbnm). (b) Magnetic ordering. The spins of the iron ions order antiferromagnetically along a . Due to the Dzyaloshinskii-Moryia interaction, a canting is induced out of the ab plane resulting in a small ferromagnetic component along c . (c) Phonons excited by the pump pulse. Singly degenerate infrared active B_{ua} and B_{ub} phonons polarized along a and b axes, respectively (calculated eigenvectors for YFeO_3). (d) The motion of the ions results in a circularly polarized phononic field due to the non-degenerate nature of the excited IR-active phonons. (e) The oscillatory decaying displacement around the equilibrium position of one of the excited B_u phonons (blue curve). The initial phase of the IR-active phonons determines the initial direction of rotation. When excited with identical phases (pump at $+45$ degrees, $B_{ub}+B_{ua}$) the ionic motion goes from linear to circular clockwise (CW) to linear (-45 degrees) and then to circular counterclockwise (CCW). The decreasing amplitude of the phonon causes the area of the loop to reduce in time. When the phonons are excited with opposite phases (pump at -45 degrees, $B_{ub}-B_{ua}$) the initial rotation is CCW.

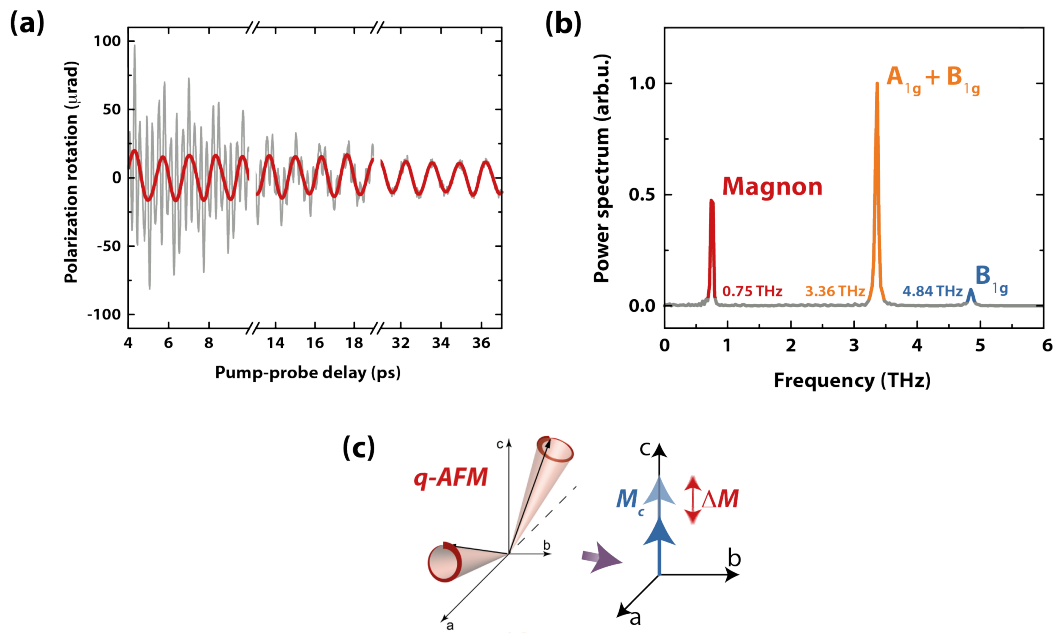


Figure 2 (a) Pump-induced changes in the polarization of the probe as a function of pump-probe delay. The slow varying component has been subtracted. Multi-component fast oscillations (grey) can be filtered out by a low pass filter (1.5 THz cut-off) to reveal the slow oscillation associated with the magnon (red). The sample was kept at 100 K while the fluence of the pump pulse was 17.6 mJ/cm². (b) Power spectrum of the oscillatory signal. The three peaks correspond to: 0.75 THz, quasi-antiferromagnetic magnon (red); 3.36 THz and 4.85 THz, Raman phonons of symmetry A_{1g}+B_{1g} (orange) and B_{1g} (blue), respectively. (c) Cartoon of the spin motion. The small ferromagnetic component along the c axis oscillates in amplitude at the magnon frequency.

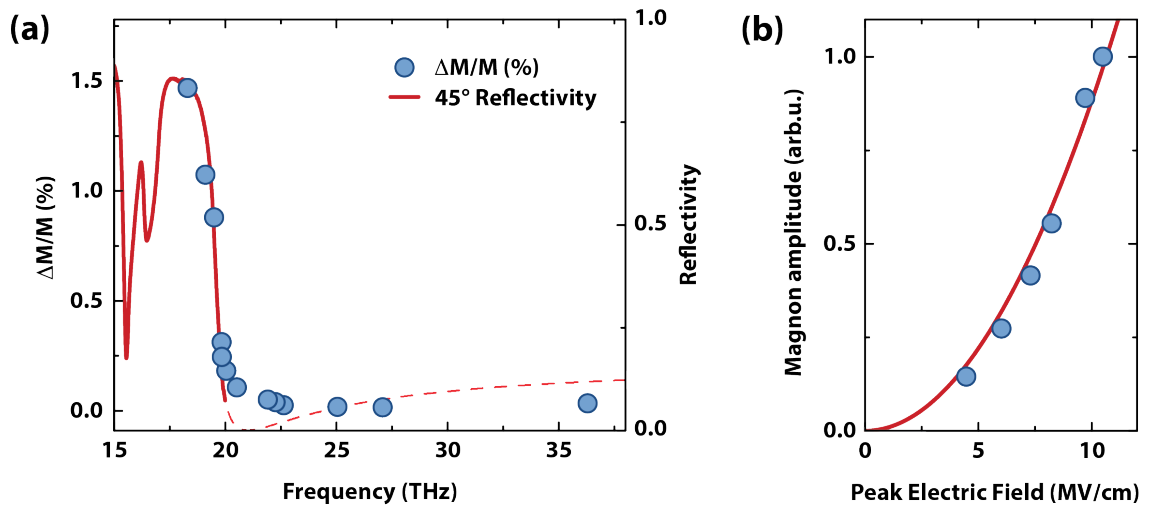


Figure 3 (a) Pump wavelength dependence of the magnetization change. The blue dots are the values of the coherent magnon amplitude derived from a fit of the oscillations and extrapolated to zero time delay. The data are corrected for the difference in penetration depth between the pump and the probe (see S5). The solid red curve is the static sample reflectivity measured by Fourier transform infrared spectroscopy (FTIR). The dashed line is a fit to the measured reflectivity. (b) Amplitude dependence on the pump field measured at 19.5 THz. The magnon amplitude scales quadratically with the pump electric field.

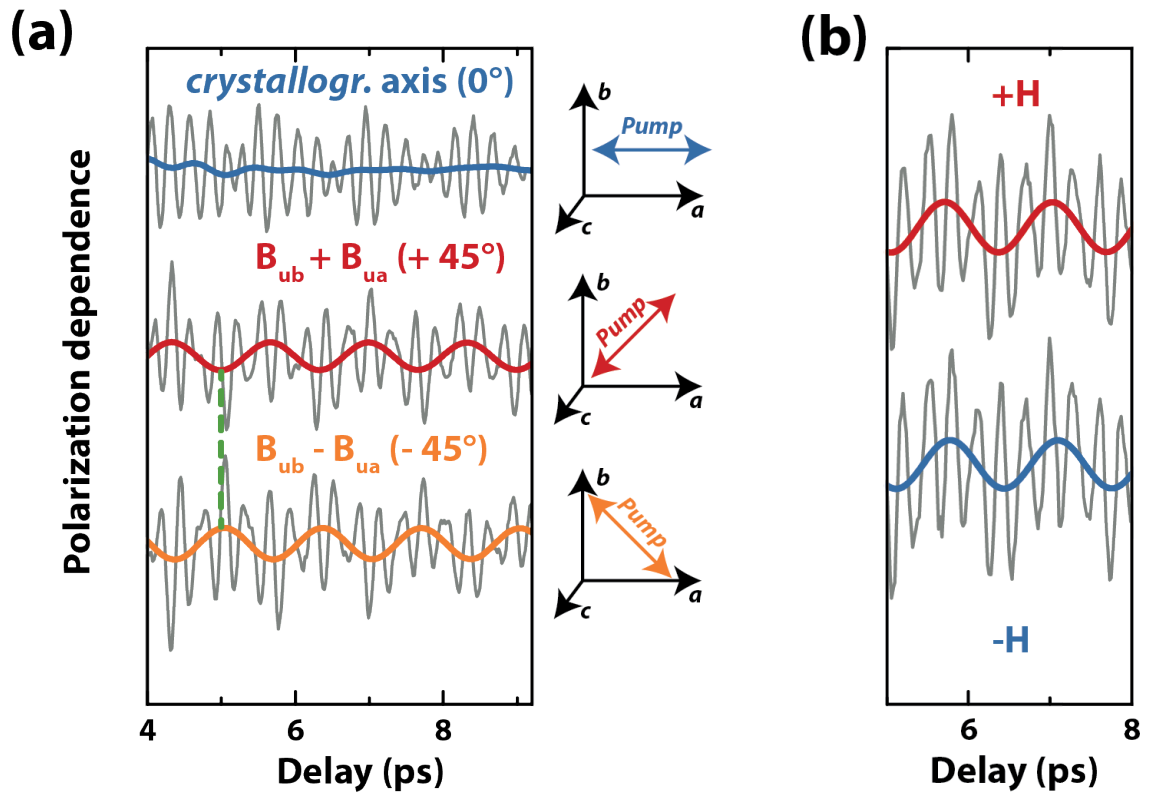


Figure 4 (a) Pump polarization dependence. Upper curve: pump polarization directed along one crystallographic axis. Only the phonon oscillations (grey) can be detected while the magnon vanishes (blue). Middle curve: pump polarization in between a and b . The two IR-active phonons are excited with the same initial positive phase ($B_{ub} + B_{ua}$). In addition to the Raman phonon oscillations (grey), the magnon appears (red). Lower curve: pump polarization rotated by 90 degrees, in between $-a$ and b . The two IR-active phonons are excited with phases of opposite signs ($B_{ub} - B_{ua}$). The magnon experiences a π phase shift (orange). (b) External magnetic field dependence. The phase of the magnon does not depend on the initial orientation of the magnetic order.

REFERENCES

-
- ⁱ Först, M. et al. Nonlinear phononics as an ultrafast route to lattice control. *Nat Phys* 7, 854 (2011).
- ⁱⁱ Rini, M. et al. Control of the electronic phase of a manganite by mode-selective vibrational excitation. *Nature* 449, 72 (2007).
- ⁱⁱⁱ Caviglia, A. D. et al. Ultrafast Strain Engineering in Complex Oxide Heterostructures. *Phys. Rev. Lett.* 108, 136801 (2012).
- ^{iv} Först, M. et al. Driving magnetic order in a manganite by ultrafast lattice excitation. *Phys. Rev. B* 84, 241104 (2011).
- ^v Först M. et al. Spatially resolved ultrafast magnetic dynamics initiated at a complex oxide heterointerface. *Nature Materials* 14, 883 (2015).
- ^{vi} Kaiser, S. et al. Optically induced coherent transport far above T_c in underdoped $\text{YBa}_2\text{Cu}_3\text{O}_{6+\delta}$. *Phys. Rev. B* 89, 184516 (2014).
- ^{vii} Hu, W. et al. Optically enhanced coherent transport in $\text{YBa}_2\text{Cu}_3\text{O}_{6.5}$ by ultrafast redistribution of interlayer coupling. *Nat Mater* 13, 705 (2014).
- ^{viii} Mitrano, M. et al. An optically stimulated superconducting-like phase in $\text{K}_3\text{C}_6\text{O}$ far above equilibrium T_c . arXiv:1505.04529 [cond-mat] (2015).
- ^{ix} Subedi, A., Cavalleri, A. & Georges, A. Theory of nonlinear phononics for coherent light control of solids. *Phys. Rev. B* 89, 220301 (2014).
- ^x Dzyaloshinskii, I. E. Thermodynamic theory of weak ferromagnetism in antiferromagnetic substances. *Sov. Phys. JETP* 5, 1259 (1957).
- ^{xi} Moriya, T. Anisotropic superexchange interaction and weak ferromagnetism. *Phys. Rev.* 120, 91 (1960).
- ^{xii} Koshizuka, N. & Ushioda, S. Inelastic-light-scattering study of magnon softening in ErFeO_3 . *Phys. Rev. B* 22, 5394 (1980).
- ^{xiii} White, R. M., Nemanich, R. J. & Herring, C. Light scattering from magnetic excitations in orthoferrites. *Phys. Rev. B* 25, 1822 (1982).
- ^{xiv} Kimel, A. V. et al. Ultrafast non-thermal control of magnetization by instantaneous photomagnetic pulses. *Nature* 435, 655 (2005).
- ^{xv} Pisarev, R. V., et al. Charge transfer transitions in multiferroic BiFeO_3 and related ferrite insulators. *Phys. Rev. B* 79 (23), 235128 (2009).
- ^{xvi} Fleury, P. A. & Loudon, R. Scattering of Light by One- and Two-Magnon Excitations. *Phys. Rev.* 166, 514 (1968).
- ^{xvii} Pershan, P. S., van der Ziel, J. P. & Malmstrom, L. D. Theoretical Discussion of the Inverse Faraday Effect, Raman Scattering, and Related Phenomena. *Phys. Rev.* 143, 574–583 (1966).
- ^{xviii} Iida, Ryugo, et al. Spectral dependence of photoinduced spin precession in DyFeO_3 . *Phys. Rev. B* 84(6), 064402 (2011).
- ^{xix} Kirilyuk, A., Kimel, A. V., & Rasing, T. Ultrafast optical manipulation of magnetic order. *Reviews of Modern Physics*, 82(3), 2731 (2010).
- ^{xx} Kubacka, T. et al. Large-Amplitude Spin Dynamics Driven by a THz Pulse in Resonance with an Electromagnon. *Science* 343, 1333 (2014).
- ^{xxi} Katsura, H., Nagaosa, N. & Balatsky, A. V. Spin Current and Magnetoelectric Effect in Noncollinear Magnets. *Phys. Rev. Lett.* 95, 057205 (2005).
- ^{xxii} Spaldin, N. A. & Fiebig, M. The Renaissance of Magnetoelectric Multiferroics. *Science* 309, 391 (2005).

-
- ^{xxiii} Abedi, A., Maitra, N. T. & Gross, E. K. U. Correlated electron-nuclear dynamics: Exact factorization of the molecular wavefunction. *The Journal of Chemical Physics* 137, 22A530 (2012).
- ^{xxiv} Min, S. K., Abedi, A., Kim, K. S. & Gross, E. K. U. Is the Molecular Berry Phase an Artifact of the Born-Oppenheimer Approximation? *Phys. Rev. Lett.* 113, 263004 (2014).
- ^{xxv} Sentef, M. A. et al. Theory of Floquet band formation and local pseudospin textures in pump-probe photoemission of graphene. *Nat Commun* 6, 7047 (2015).